

RESEARCH

Open Access



# Wine- and stir-frying processing of Cuscutae Semen enhance its ability to alleviate oxidative stress and apoptosis via the Keap 1-Nrf2/HO-1 and PI3K/AKT pathways in H<sub>2</sub>O<sub>2</sub>-challenged KGN human granulosa cell line

Yusha Liang<sup>1†</sup>, Yun Shi<sup>1†</sup>, Rong Guo<sup>1†</sup>, Changli Xu<sup>2</sup>, Mian Fu<sup>1</sup>, Jinyang Shen<sup>1</sup>, Xun Gao<sup>1\*</sup>, Weidong Li<sup>3\*</sup> and Kunming Qin<sup>1\*</sup>

## Abstract

**Background** Cuscutae Semen (CS) has been prescribed in traditional Chinese medicine (TCM) for millennia as an aging inhibitor, an anti-inflammatory agent, a pain reliever, and an aphrodisiac. Its three main forms include crude Cuscutae Semen (CCS), wine-processed CS (WCS), and stir-frying-processed CS (SFCS). Premature ovarian insufficiency (POI) is a globally occurring medical condition. The present work sought a highly efficacious multi-target therapeutic approach against POI with minimal side effects. Finally, it analyzed the relative differences among CCS, WCS and SFCS in terms of their therapeutic efficacy and modes of action against H<sub>2</sub>O<sub>2</sub>-challenged KGN human granulosa cell line.

**Methods** In this study, ultrahigh-performance liquid chromatography (UPLC)-Q-Exactive<sup>TM</sup> Orbitrap-mass spectrometry (MS), oxidative stress indices, reactive oxygen species (ROS), Mitochondrial membrane potential (MMP), real-time PCR, Western blotting, and molecular docking were used to investigate the protective effect of CCS, WCS and SFCS on KGN cells oxidative stress and apoptosis mechanisms.

**Results** The results confirmed that pretreatment with CCS, WCS and SFCS reduced H<sub>2</sub>O<sub>2</sub>-induced oxidative damage, accompanied by declining ROS levels and malondialdehyde (MDA) accumulation in the KGN cells. CCS, WCS and SFCS upregulated the expression of antioxidative levels (GSH, GSH/GSSG ratio, SOD, T-AOC), mitochondrial membrane potential (MMP) and the relative mRNA (Nrf2, Keap1, NQO-1, HO-1, SOD-1, CAT). They inhibited apoptosis by upregulating Bcl-2, downregulating Bax, cleaved caspase-9, and cleaved caspase-3, and lowering the Bax/Bcl-2 ratio. They also exerted antioxidant efficacy by partially activating the PI3K/Akt and Keap1-Nrf2/HO-1 signaling pathways.

<sup>†</sup>Yusha Liang, Yun Shi and Rong Guo contributed equally to this work.

\*Correspondence:

Xun Gao

731594078@qq.com

Weidong Li

liweidong0801@163.com

Kunming Qin

qinkm123@126.com

Full list of author information is available at the end of the article



**Conclusions** The results of the present work demonstrated the inhibitory efficacy of CCS, WCS and SFCS against H<sub>2</sub>O<sub>2</sub>-induced oxidative stress and apoptosis in KGN cells and showed that the associated mechanisms included Keap1-Nrf2/HO-1 activation, P-PI3K upregulation, and P-Akt-mediated PI3K-Akt pathway induction.

**Keywords** Crude Cuscutae Semen (CCS), Wine-processed Cuscutae Semen (WCS), Stir-frying-processed Cuscutae Semen (SFCS), Human granulosa cell line KGN, Premature ovarian insufficiency (POI), Oxidative stress, Apoptosis

## Background

In premature ovarian insufficiency (POI), the ovarian reserve is depleted before the age of 40 years. This disorder is characterized by sterility, amenorrhea or oligomenorrhea, hypoestrogenism, and elevated serum follicle-stimulating hormone (FSH) levels (> 25 mIU/mL). Women suffering from prolonged POI are at increased risk of cardiovascular diseases (CVDs), neurological impairment, psychological dysfunction, and osteoporosis [1]. The granulosa cell layer in the follicles mediates metabolism, material transport, and signal transduction in oocytes. Granulosa cells also play vital roles in follicular growth, proliferation, differentiation, atresia/ovulation, and corpus luteum formation [2]. Granulosa cell quality influences female fertility [3]. However, no efficacious therapies are currently available for POI, and the pathogenesis of this disorder remains poorly understood.

Cuscutae Semen (CS) has been prescribed in traditional Chinese medicine (TCM) for millennia. As wine- and stir-frying-processing alter the pharmaceutical effects of CS, these modified forms of the medicine have been administered for applications that clinically differ from those of CS. The earliest known record of Cuscutae Semen (CS; dry mature seeds of *Cuscuta australis* R. Br. or *Cuscuta chinensis* Lam.; family Convolvulaceae) dates back to the “Agriculture God’s Canon of Materia Medica” ca. 2,000 years ago. In this text, CS was designated a superior-grade drug. Presently, it is widely employed in Traditional Chinese Medicine (TCM) practices to nourish vital organs such as liver and kidney, treat impotence and seminal emission, prevent miscarriage, and enhance vision [4, 5]. Modern pharmacological experimentation demonstrated that CS reverses reductions in testosterone levels and androgen receptor gene expression, is immunomodulatory, hepatoprotective, antioxidant, anti-inflammatory, and anti-aging, and enhances memory by inducing PC12 cell differentiation [6–8]. Prior research showed that CCS supplementation invigorates internal organs such as the kidneys, and salt pretreatment potentiates it [9]. Our previous study indicated that heating transformed CCS into SFCS, and a hierarchical cluster analysis (HCA) clearly distinguished them both. A principal component analysis (PCA) disclosed that the levels of neochlorogenic acid, cryptophyllogenic acid, caffeic acid, quercetin, isorhamnetin, and kaempferol significantly

differed between CCS and SFCS [10]. Though stir-frying adjusted the curative effect of CS, it was nonetheless difficult to distinguish among crude Cuscutae Semen (CCS), wine-processed Cuscutae Semen (WCS), and stir-frying-processed Cuscutae Semen (SFCS) in clinical practice. Moreover, little is known about the impact of CCS, WCS and SFCS on oxidative stress and apoptosis in POI. In 2023, the latest research shows that Dingkun Pill modulate ovarian function in premature ovarian insufficiency mice by regulating PI3K/AKT signaling pathway [11]. It also laid a foundation for the mechanism and target of treatment of premature ovarian failure before and after CS processing.

Reactive oxygen species (ROS) are the major chemical mediators of oxidative stress. Low ROS levels are essential for certain biological functions such as ovulation and luteolysis [12]. Nevertheless, excessive ROS production is detrimental to cell function and is associated with various human diseases such as diabetes [13], CVDs [14], and neuropathies [15]. POI is characterized by elevated serum ROS and oxidative stress marker levels [16, 17]. Severe oxidative stress may impair ovarian function [18]. However, the roles of oxidative stress in the etiology of POI have received limited research attention. The granulosa-like tumor cell line designated KGN is steroidogenic and is regarded as a reliable in vitro model of human granulosa cells [19]. H<sub>2</sub>O<sub>2</sub>-challenged KGN cells have been extensively used for in vitro experimentation involving POI [20].

Oxidative stress occurs when there is an elevated ratio of oxidants to antioxidants resulting in the disruption of redox signaling and the induction of molecular and cellular damage [21]. As excessive ROS cannot be eliminated fast enough, they can accumulate and interfere with the normal cellular redox state [22]. *N*-acetylcysteine (NAC) has mucolytic efficacy and potent antioxidant activity. It stimulates glutathione biosynthesis, promotes detoxification, and scavenges free radicals [23]. Oxidant and antioxidant systems are in dynamic equilibrium under normal physiological conditions. The antioxidant system consists of enzymes such as superoxide dismutase (SOD) and catalase (CAT) as well as non-enzymatic substances including glutathione (GSH), oxidized glutathione disulfide (GSSG), melatonin, ascorbic acid (vitamin C), vitamin E (mixed tocopherols), and copper, zinc, and

selenium cations. The total antioxidant capacity (T-AOC) is another important indicator of redox balance. When ROS are overproduced or antioxidant biosynthesis decreases, the redox reactions go into dysequilibrium and the body enters oxidative stress (OS) [24]. OS causes pathological damage to the ovarian microenvironment including meiotic arrest in the oocytes, granulosa cell apoptosis, corpus luteum dysfunction, and accelerated ovary aging. However, antioxidant supplementation improves the OS and ovary function.

Antioxidant systems respond to the oxidative damage caused by ROS via several signaling pathways. Nuclear factor (erythroid-derived 2)-like 2 (Nrf2) is a major transcription factor (TF) associated with the oxidative stress response [25, 26]. Nrf2 is a member of the Cap'n'Collar (CNC) subfamily of basic leucine zipper (bZIP) TFs. It comprises seven conserved Nrf2-ECH homology (Neh) domains with different functions including the modulation of Nrf2 stability and contribution to the central role of Nrf2 in the redox system. Kelch-like-ECH-associated protein 1 (Keap1) regulates Nrf2 activity. In steady-state, Keap1 binds Nrf2 via its C-terminal domain and anchors it in the cytoplasm at a low basal protein level. The resultant Keap1-Cullin (CUL) 3-RING-box protein mediates Nrf2 ubiquitination and degradation via the 26S proteasome [27]. Oxidative stress inactivates Keap1, and newly synthesized Nrf2 translocates to the nucleus where it induces the transcription of antioxidant heme oxygenase 1 (HO-1) and quinone oxidoreductase 1 (NQO1) genes [28]. The mechanism by which oxidative stress activates Nrf2 is unknown. Nevertheless, a few earlier studies showed that upstream phosphatidylinositol-3-kinase (PI3K)/Akt activates Nrf2 and its downstream proteins such as HO-1 [29, 30].

The present study aimed to (1) establish whether CCS, WCS and SFCS inhibit oxidative stress and apoptosis in H<sub>2</sub>O<sub>2</sub>-challenged KGN cells and (2) elucidate their modes of action in POI treatment.

## Material and methods

### Materials and reagents

The materials used in this study included *Cuscuta Semen* (No. 20201201; Anhui Tonghuatang Chinese Herbal Decoction Pieces Co. Ltd., Anhui, China), *N*-acetylcysteine (NAC; No. ST1546, Beyotime Biotechnology, Shanghai, China), H<sub>2</sub>O<sub>2</sub> (No. 20201201, Shanghai Sell-eck Chemicals Co. Ltd., Shanghai, China), fetal bovine serum (FBS; (No. 164210–500, Procell Life Science & Technology Co. Ltd., Wuhan, China), Dulbecco's modified Eagles's medium/F12 medium (DMEM/F12; No. VCM12500, VICMED, Xuzhou, China), Cell Counting Kit-8 (CCK-8; No. C6005; NCM Biotech, Suzhou, China), ROS Detection Kit (No. S0033S; Beyotime

Biotechnology), Malondialdehyde (MDA) Assay Kit (No. S0131S; Beyotime Biotechnology), Enhanced Bicinchoninic Acid (BCA) Protein Assay Kit (No. P0010; Beyotime Biotechnology), Superoxide Dismutase (SOD) Assay Kit (No. S0109; Beyotime Biotechnology), Glutathione (GSH) and Oxidized Glutathione (GSSG) Assay Kit (No. S0053; Beyotime Biotechnology), Mitochondrial Membrane Potential with Mito<sup>®</sup> Tracker Red CMXRos (No. C1071S; Beyotime Biotechnology), Total Antioxidant Capacity Assay Kit (No. AK351; Bioss Inc., Beijing, China), TRIzol reagent (No. R401-01; Vazyme Biotech, Shanghai, China), RT Master Mix for qPCR II (No. HY-K0511A; Med-ChemExpress (MCE), Monmouth Junction, NJ, USA), SYBR Green Real MasterMix (No. HY-K0523; MCE) The primary antibodies anti-Keap 1 (No. TA5266F), anti-NQO1 (No. T56710F), anti-Bcl-2 (No. T40056F), anti-Nrf2 (No. T55136F), anti-HO 1 (No. T55113F), anti-Bax (No. T40051F), anti-PI3K/p85- $\alpha$  (Nos. T40115F and T40116F), anti-phospho-Akt (Ser473) (No. T40067F), anti-Akt1/2/3 (No. T55561F), and anti-PI3K/p85- $\alpha$  (T40115F) were purchased from Abmart (Berkeley Heights, NJ, USA). The primary antibodies anti-SOD2 (No. WL02506), anti-cleaved caspase-9 (No. WL01838), and anti-cleaved caspase 3 (No. WL02117) were purchased from Wanlei Biotechnology Co. Ltd. (Shanghai, China). The primary antibody anti- $\beta$ -actin (No. 66009–1-Ig) was purchased from Proteintech Group (Rosemont, IL, USA). The secondary antibodies anti-rabbit immunoglobulin G (IgG) (H+L) (No. SA00001-2) and anti-mouse IgG (H+L) (No. SA00001-1) were purchased from Proteintech Group.

### CCS, WCS and SFCS extract processing

One-half gram (0.5 g) of each of the CCS, WCS and SFCS powders was precisely weighed out, extracted by ultrasonication with 20 mL of 80% (v/v) ethanol for 30 min, and centrifuged at 13,000 rpm for 5 min. Each solution was then transferred to a 25-mL volumetric flask and the volume was made up to the mark with 80% (v/v) methanol. Each solution was then concentrated and freeze-dried to powder under vacuum and each powder was stored at -80 °C until the subsequent experiments.

### Ultrahigh-performance Q-exactive<sup>™</sup> mass spectrometry (UPLC-Q-Exactive<sup>™</sup> Orbitrap-MS)

UPLC-Q-Exactive<sup>™</sup> Orbitrap-MS was conducted in a Thermo Fisher U3000 UPLC fitted with an online degasser, a quaternary gradient pump, a column temperature chamber, an automatic sampler, and a Q Exactive<sup>™</sup> Plus Orbitrap ionization source (Thermo Fisher Scientific, Waltham, MA, USA). Chromatographic separation was performed with a Waters ACQUITY UPLC HSS T3 C18 column (2.1 mm  $\times$  100 mm, 1.8  $\mu$ m; Waters Corporation,

Milford, MA, USA). UV detection of the UHPLC fractions was executed with a U3000 3D field DAD detector. The analytical column temperature was fixed at 35 °C, and the injection volume was 10 µL. Gradient elution was performed using 0.1% (v/v) formic acid in water (solvent A) and acetonitrile (solvent B). The flow rate was set to 0.3 mL/min, and the gradient elution program was as follows: 0–10 min, 100% A; 10–25 min, 70–60% A; 25–30 min, 60–50% A; 30–40 min, 50–30% A; 40–45 min, 30–0%; 45–60 min, 0% A; 60–60.5 min, 0–100% A; 60.5–70 min, 100% A. For the MS, the positive and negative ion modes were in the range of  $m/z$  100–1,200, the sheath and auxiliary gas flow rates were 40 arb and 15 arb, respectively, the capillary and Aux gas heater temperatures were 320 °C and 350 °C, respectively, the positive spray voltage was 3.2 kV, and the MS and MS/MS resolutions were 70,000 and 17,500, respectively. A *Cuscutae Semen* composition database was established based on a literature review and a TCM natural products database to summarize and analyze the unknown substances in CCS, WCS and SFCS.

#### Cell culture and treatment

The human ovarian granule KGN cell line was purchased from Punosai Company (Wuhan, China) and cultured in DMEM/F12 medium containing 100 U/mL penicillin, streptomycin, and 10% (v/v) FBS in an incubator at 37 °C, 75% RH, and 5% CO<sub>2</sub>. The groups to which the KGN cells were assigned included the normal control (CON); model (MOD, 400 µM H<sub>2</sub>O<sub>2</sub>); positive control (NAC, 5 mM NAC+400 µM H<sub>2</sub>O<sub>2</sub>); crude CS (CCS, 0.1 mg/mL CS extract+400 µM H<sub>2</sub>O<sub>2</sub> and 0.3 mg/mL CS extract+400 µM H<sub>2</sub>O<sub>2</sub>), CCS low-dose (CCS-L, 0.1 mg/mL), CCS high-dose (CCS-H, 0.3 mg/mL); wine-processed CS (WCS, 0.1 mg/mL WCS extract+400 µM H<sub>2</sub>O<sub>2</sub> and 0.3 mg/mL WCS extract+400 µM H<sub>2</sub>O<sub>2</sub>), WCS low-dose (WCS-L, 0.1 mg/mL), WCS high-dose (WCS-H, 0.3 mg/mL); stir-frying-processed CS (SFCS, 0.1 mg/mL SFCS extract+400 µM H<sub>2</sub>O<sub>2</sub> and 0.3 mg/mL SFCS extract+400 µM H<sub>2</sub>O<sub>2</sub>), SFCS low-dose (SFCS-L, 0.1 mg/mL), and SFCS high-dose (SFCS-H, 0.3 mg/mL).

#### Cell viability assay

KGN cells were seeded in 96-well flat-bottomed plates at  $4 \times 10^4$ /well and exposed to various CCS, WCS and SFCS concentrations for 24 h to establish the safe CCS, WCS and SFCS concentration range. The cells were then treated with different H<sub>2</sub>O<sub>2</sub> concentrations for 2 h to determine the safe H<sub>2</sub>O<sub>2</sub> exposure range. KGN cells were then seeded in 96-well plates at  $4 \times 10^4$ /well and subjected to CCS, WCS, SFCS, and NAC for 24 h and then to H<sub>2</sub>O<sub>2</sub> for 2 h. Cell viability was then measured with a CCK-8 Kit and an inverted microscope.

#### MDA, SOD, T-AOC, GSH, GR, and GSSG measurements

Peroxidation of the KGN cell membrane lipids was assessed by measuring MDA production. The antioxidant ability was evaluated by detecting SOD, T-AOC, GSH, GSSG, and GR using commercially available kits and according to the manufacturers' instructions.

#### Intracellular ROS measurement

Intracellular ROS was measured with the ROS Assay Kit according to the manufacturer's protocol. KGN cells exposed to CCS, WCS, SFCS, NAC, H<sub>2</sub>O<sub>2</sub> and active oxygen-positive (AOP) were incubated with 10 µM of the 2',7'-dichlorofluorescein diacetate (DCFH-DA) fluorescent probe at 37 °C for 30 min, washed twice with pre-cooled phosphate-buffered saline (PBS), and photographed under a fluorescence microscope.

#### Mitochondrial membrane potential detection

KGN cell apoptosis was detected with Mito<sup>®</sup> Tracker Red CMXRos (No. C1071S; Beyotime Biotechnology). The treated KGN cells were collected in 0.25% (w/v) trypsin (No. VC2004; VICMED), washed twice with PBS, resuspended in 188 µL PBS, incubated with 2 µL Mito<sup>®</sup> Tracker Red CMXRos and 5 µL Hoechst33342 in the dark at 37 °C for 30 min, quantified with ImageJ software (National Institutes of Health [NIH], Bethesda, MD, USA), and photographed under a fluorescence microscope.

#### Gene expression analysis

TRIzol reagent (Vazyme Biotech) was used to extract the RNA from the KGN cells. RNA purity and concentration were measured in a NanoDrop 2000 spectrophotometer (Thermo Fisher Scientific). DNA was removed with RNase-Free DNase (MCE) and the RNA was reverse-transcribed to cDNA with MonScript RTIII Super Mix (MCE). The output was then statistically analyzed in a Step One Plus Detection System (Thermo Fisher Scientific). The data acquired were based on β-actin as the internal reference, and the relative gene expression levels were computed by the  $2^{-\Delta\Delta Ct}$  method. The specific primers used are listed in Table 1.

#### Western blotting

KGN cells were lysed with radioimmunoprecipitation (RIPA) buffer supplemented with phenylmethanesulfonyl fluoride (PMSF) and centrifuged at 12,000 rpm and 4 °C for 10 min. The protein concentration in the samples was detected by the BCA method (Beyotime Biotechnology). The proteins were separated by sodium dodecyl sulfate–polyacrylamide gel electrophoresis (SDS-PAGE) and transferred to a polyvinylidene difluoride (PVDF) membrane (EMD Millipore, Billerica, MA, USA). Each

**Table 1** Primer sequences used in Real-Time PCR analyses

Gene	Forward Sequence	Reverse Sequence	NCBI No
Nrf2	TCACACGAGATGAGCTTAGGGCAA	TACAGTTCTGGCGGCGACTTTAT	NM_010902.4
Keap1	CAGCAACTCTGTGACGTGACC	TCAATAAGCCTTTCCATGACCT	NM_016679.4
SOD1	TGGTTTGCCTGCTAGTCTCC	CTTCGTCGCCATAACTCGCT	NM_000454.4
HO-1	ATGGCCTCCCTGTACCACATC	TGTTGCGCTCAATCTCCTCT	NM_002133.2
CAT	CCATTATAAGACTGACCAGGGC	AGTCCAGGAGGGGTACTTTCC	NM_001752.3
Bcl-2	ATGTGTGTGGAGCGTCAACC	CAGAGACAGCCAGGAGAAATC	NM_000633.3
Bax	GAGCTGCAGAGGATGATTGCT	TGATCAGCTCGGGCACTTTA	NM_007527.3
$\beta$ -actin	CAAGAGAGGTATCCTGACCT	TGATCTGGGTACATCTTTTAC	NM_007393.5

membrane was blocked, incubated at 4 °C overnight with the aforementioned primary antibodies, and probed with horseradish peroxidase (HRP)-conjugated secondary antibody at room temperature for 1 h. An enhanced chemiluminescence (ECL) system (VICMED) and luminous solution were used to detect fluorescent bands in an imager, and the bands were quantitatively analyzed with ImageJ software.

#### Statistical analysis

All data were analyzed with GraphPad Prism v. 9.5 (GraphPad Software, La Jolla, CA, USA) and presented as means  $\pm$  standard deviation (SD). Multiple comparisons were made via one-way analysis of variance (ANOVA) followed by Tukey's post-hoc test.  $P < 0.01$  or  $P < 0.05$  indicated a statistically significant difference.

## Results

### Chemical constituents of CCS, WCS and SFCS

UPLC-Q-Exactive<sup>TM</sup> Orbitrap-MS was used to analyze the CCS, WCS and SFCS extracts. Total ion chromatograms in negative and positive ion modes for CCS, WCS and SFCS are shown in Fig. 1A–E. The five major bioactive compounds were identified as rutin, chlorogenic acid, astragaloside, isoquercitrin, and hyperoside (Fig. 1G). The top 30 ingredients were detected in CCS, WCS and SFCS, and they included mainly flavonoids, phenolic acids, and lignans. They are listed in Table 2 and the last 51 ingredients were listed in Supplementary Material 1.

### Effects of CCS, WCS and SFCS on KGN cell viability

The effects of CCS, WCS, SFCS, NAC, and H<sub>2</sub>O<sub>2</sub> on KGN cell viability were evaluated by CCK-8 assay. At 0.1–0.7 mg/mL, CCS, WCS and SFCS were not cytotoxic to KGN cells compared to the control. At 0.8 mg/mL, however, CCS was not cytotoxic but WCS and SFCS were significantly cytotoxic to KGN cells (Fig. 2C–E). KGN cells were subjected to various H<sub>2</sub>O<sub>2</sub> concentrations (0–600  $\mu$ M), and the one inducing oxidative damage was determined. Figure 2B

shows that 400  $\mu$ M H<sub>2</sub>O<sub>2</sub> decreased KGN cell viability to ~40%. Hence, this H<sub>2</sub>O<sub>2</sub> concentration was selected for the subsequent experiments. Figure 2F shows that pretreatment with CCS, WCS, SFCS, and NAC for 24 h alleviated damage to H<sub>2</sub>O<sub>2</sub>-challenged KGN cells. KGN cells were co-treated with 400  $\mu$ M H<sub>2</sub>O<sub>2</sub> and either 0.1 mg/mL or 0.3 mg/mL CCS, WCS and SFCS as well as 5 mM NAC. While both concentrations of CCS, WCS and SFCS alleviated injury to H<sub>2</sub>O<sub>2</sub>-challenged KGN cells at 24 h. Microscopic examination confirmed that CCS, WCS, SFCS, and NAC inhibited morphological damage to H<sub>2</sub>O<sub>2</sub>-challenged KGN cells (Fig. 2A). Moreover, WCS and SFCS exerted a stronger protective effect than CCS against H<sub>2</sub>O<sub>2</sub>-induced damage in KGN cells.

### CCS, WCS and SFCS decreased MDA and GSSG but increased T-AOC, SOD, GSH, GR, and GSH/GSSG ratio in H<sub>2</sub>O<sub>2</sub>-challenged KGN cells

The observed changes in the MDA, T-AOC, SOD, GSH, GR, and GSSG levels and the GSH/GSSG ratio in the KGN cells indicated that H<sub>2</sub>O<sub>2</sub> exposure induced oxidative stress in them. In the MOD group, the MDA and GSSG levels had increased while SOD, T-AOC, GSH, and GR activity and the GSH/GSSG ratio had decreased compared to the CON group. However, the foregoing abnormal changes were partially rescued in response to the NAC, CCS, WCS and SFCS treatments. NAC and high concentrations of WCS and SFCS effectively attenuated the adverse effects of oxidative stress in the MOD group (Fig. 3A–G). The preceding results suggest that NAC inhibited oxidative stress in H<sub>2</sub>O<sub>2</sub>-challenged KGN cells while WCS and SFCS more effectively mitigated the inhibitory effect of oxidative stress on KGN cells than CCS. Hence, wine- and stir-frying processing enhance the antioxidant capacity of CS.

### CCS, WCS and SFCS increased mitochondrial activity in H<sub>2</sub>O<sub>2</sub>-challenged KGN cells

Abnormal ROS accumulation was observed in KGN cells exposed to H<sub>2</sub>O<sub>2</sub>. The fluorescence intensity was significantly higher in the H<sub>2</sub>O<sub>2</sub>-challenged KGN cells

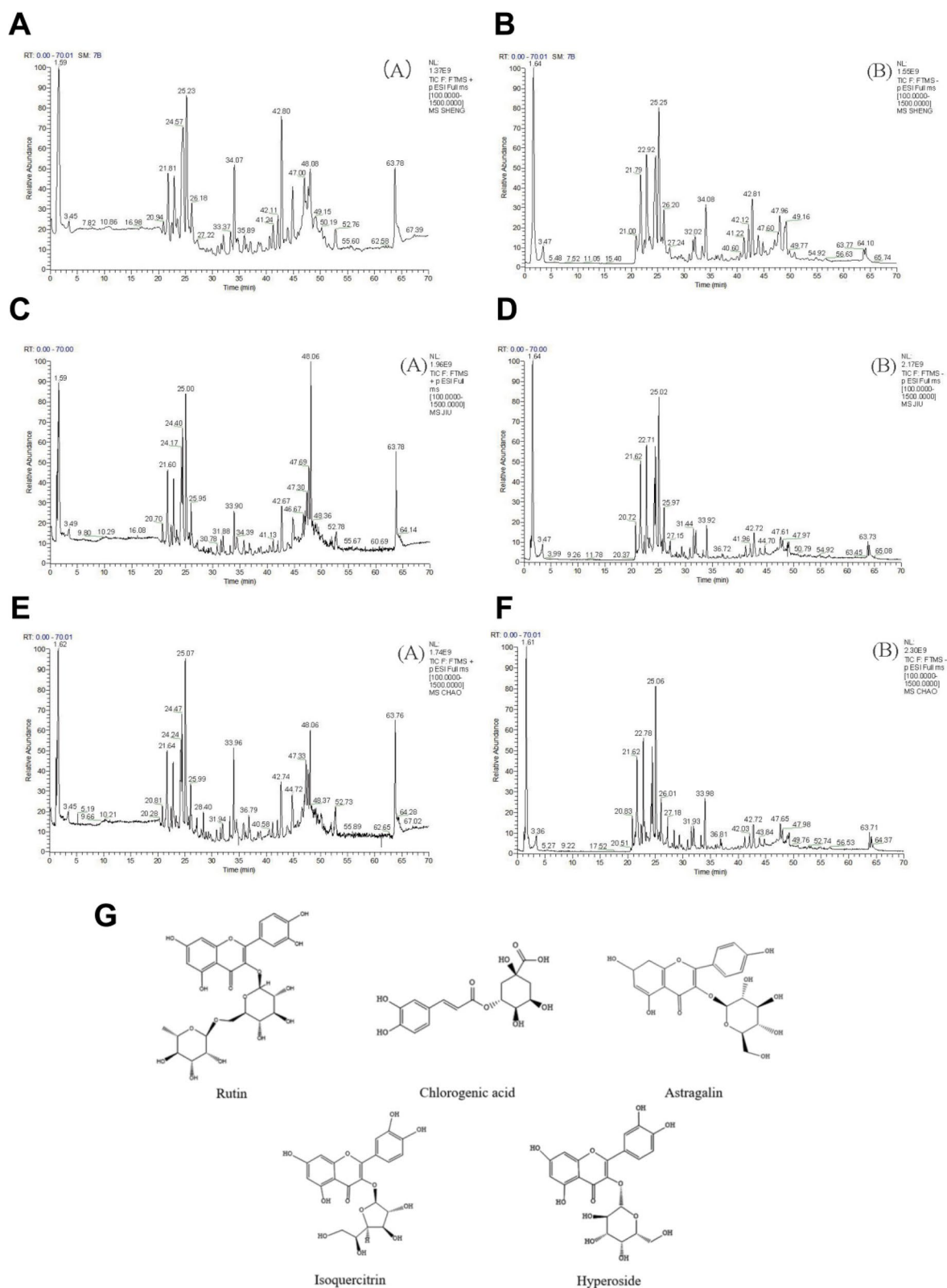


**Fig. 1** Chemical constituents in CCS, WCS, and SFCS. **A, B** Total ion chromatogram of CCS extracts in positive **(A)** and negative **(B)** ion mode. **C, D** Total ion chromatogram of WCS extracts in positive **(A)** and negative **(B)** ion mode. **E, F** Total ion chromatogram of SFCS extracts in positive **(A)** and negative **(B)** ion mode. **G** Chemical structures of CCS, WCS, and SFCS

**Table 2** Principal component identifications of different processed products of Cuscuta Semen

No	Identification	Formula	theoretical value(m/z)	Error (ppm)	tR/min	Source	Quasi-molecular ion
1	Kaempferol	C <sub>15</sub> H <sub>10</sub> O <sub>6</sub>	286.0477	-0.15	31.51	CCS,WCS,SFCS	[M-H] <sup>-</sup>
2	Astragalin	C <sub>21</sub> H <sub>20</sub> O <sub>11</sub>	448.1006	-0.02	26.01	CCS,WCS,SFCS	[M-H] <sup>-</sup>
3	Isorhamnetin	C <sub>16</sub> H <sub>12</sub> O <sub>7</sub>	316.0583	0.05	31.85	CCS,WCS,SFCS	[M-H] <sup>-</sup>
4	Hyperoside	C <sub>21</sub> H <sub>20</sub> O <sub>12</sub>	464.0955	0.13	25.09	CCS,WCS,SFCS	[M-H] <sup>-</sup>
5	Quercetin	C <sub>15</sub> H <sub>10</sub> O <sub>7</sub>	302.0426	-0.2	29.34	CCS,WCS,SFCS	[M-H] <sup>-</sup>
6	Isochlorogenic acid C	C <sub>25</sub> H <sub>24</sub> O <sub>12</sub>	516.1268	0.12	26.40	CCS,WCS,SFCS	[M-H] <sup>-</sup>
7	Chlorogenic acid	C <sub>16</sub> H <sub>18</sub> O <sub>9</sub>	354.0950	-0.35	21.82	CCS,WCS,SFCS	[M-H] <sup>-</sup>
8	Cryptochlorogenic acid	C <sub>16</sub> H <sub>18</sub> O <sub>9</sub>	354.0950	-0.25	22.77	CCS,WCS,SFCS	[M+H] <sup>+</sup>
9	Quinic acid	C <sub>7</sub> H <sub>12</sub> O <sub>6</sub>	192.0633	-0.24	22.78	CCS,WCS,SFCS	[M+H] <sup>+</sup>
10	Isochlorogenic acid B	C <sub>25</sub> H <sub>24</sub> O <sub>12</sub>	516.1269	0.14	25.52	WCS,SFCS	[M+H] <sup>+</sup>
11	Caffeic acid	C <sub>9</sub> H <sub>8</sub> O <sub>4</sub>	180.0423	0.03	22.80	CCS,WCS,SFCS	[M+H] <sup>+</sup>
12	Neochlorogenic acid	C <sub>16</sub> H <sub>18</sub> O <sub>9</sub>	354.0951	-0.09	25.53	CCS,WCS,SFCS	[M+H] <sup>+</sup>
13	Apigenin	C <sub>15</sub> H <sub>10</sub> O <sub>5</sub>	270.0529	0.13	31.16	CCS,WCS,SFCS	[M-H] <sup>-</sup>
14	Pinoresinol	C <sub>26</sub> H <sub>32</sub> O <sub>11</sub>	520.1947	0.42	25.60	CCS,WCS,SFCS	[M+H] <sup>+</sup>
15	Ferulic acid	C <sub>10</sub> H <sub>10</sub> O <sub>4</sub>	194.0579	0.16	25.50	CCS,WCS,SFCS	[M+H] <sup>+</sup>
16	Manninotriose	C <sub>18</sub> H <sub>32</sub> O <sub>16</sub>	504.1691	0.17	1.68	CCS,WCS,SFCS	[M+H] <sup>+</sup>
17	p-Coumaric acid	C <sub>9</sub> H <sub>8</sub> O <sub>3</sub>	164.0475	0.66	24.90	CCS,WCS,SFCS	[M+H] <sup>+</sup>
18	Gallic acid	C <sub>7</sub> H <sub>6</sub> O <sub>5</sub>	170.0216	0.15	27.66	CCS,WCS,SFCS	[M+H] <sup>+</sup>
19	Abscisic acid	C <sub>15</sub> H <sub>20</sub> O <sub>4</sub>	264.1362	0.01	28.61	CCS,WCS,SFCS	[M-H] <sup>-</sup>
20	Arglabin	C <sub>15</sub> H <sub>18</sub> O <sub>3</sub>	246.1256	0.07	25.58	CCS,WCS,SFCS	[M+H] <sup>+</sup>
21	(+)-Pinoresinol	C <sub>20</sub> H <sub>22</sub> O <sub>6</sub>	358.1416	-0.21	25.60	CCS,WCS,SFCS	[M-H] <sup>+</sup>
22	Abietic acid	C <sub>20</sub> H <sub>30</sub> O <sub>2</sub>	302.2245	-0.27	47.45	WCS,SFCS	[M+H] <sup>+</sup>
23	Gentiopicroin	C <sub>16</sub> H <sub>20</sub> O <sub>9</sub>	356.1108	0.09	22.47	CCS,WCS,SFCS	[M+H] <sup>+</sup>
24	2-Hydroxy-4-methoxybenzaldehyde	C <sub>8</sub> H <sub>8</sub> O <sub>3</sub>	152.0474	0.50	24.78	CCS,WCS,SFCS	[M+H] <sup>+</sup>
25	Daidzin	C <sub>21</sub> H <sub>20</sub> O <sub>9</sub>	416.1106	-0.39	24.09	CCS,WCS,SFCS	[M+H] <sup>+</sup>
26	4-Hydroxybenzoic acid	C <sub>7</sub> H <sub>6</sub> O <sub>3</sub>	138.0317	0.11	22.30	CCS,WCS,SFCS	[M+H] <sup>+</sup>
27	Naringenin	C <sub>15</sub> H <sub>12</sub> O <sub>5</sub>	272.0684	-0.13	30.93	CCS,WCS,SFCS	[M+H] <sup>+</sup>
28	Daidzein	C <sub>15</sub> H <sub>10</sub> O <sub>4</sub>	254.0579	-0.11	28.49	CCS,WCS,SFCS	[M+H] <sup>+</sup>
29	Arbutin	C <sub>12</sub> H <sub>16</sub> O <sub>7</sub>	272.0898	0.68	6.26	CCS,SFCS	[M+H] <sup>+</sup>
30	Glycitein	C <sub>16</sub> H <sub>12</sub> O <sub>5</sub>	284.0684	-0.42	28.89	CCS,WCS,SFCS	[M+H] <sup>+</sup>

than in the untreated control. Pretreatment with NAC, WCS-H, and SFCS-H markedly decreased intracellular ROS whereas AOP, CCS-L, CCS-H, WCS-L, and SFCS-L had minimal impact on it (Fig. 4C and D).

The loss of mitochondrial membrane potential (MMP) in response to H<sub>2</sub>O<sub>2</sub>-induced cytotoxicity was measured by a Mito<sup>®</sup> Tracker Red CMXRos assay. A decrease in MMP indicates apoptosis. Figure 4A–B show that Mito<sup>®</sup> Tracker Red CMXRos aggregated and emitted red fluorescence in the CON group. The ratio of red/blue fluorescent positive cells was greatly decreased after H<sub>2</sub>O<sub>2</sub> exposure, and pretreatments with CCS, WCS and SFCS significantly increased the ratio in a dose-dependent manner.

#### Regulation of apoptosis-related protein and gene levels in H<sub>2</sub>O<sub>2</sub>-challenged KGN cells by CCS, WCS and SFCS

Various stressors cause mitochondrial outer membrane permeabilization (MOMP), thereby initiating mitochondrial apoptosis. The expression levels of the aforementioned apoptosis-related proteins and their corresponding genes were assessed to determine the effects of CCS, WCS and SFCS on KGN cells. The levels of pro-apoptotic Bax, cleaved caspase-9, and cleaved caspase-3 were lower while the level of anti-apoptotic Bcl-2 was higher in the KGN cells treated with CCS, WCS and SFCS than in those challenged with H<sub>2</sub>O<sub>2</sub>, and the magnitudes of these differences were dose-dependent (Fig. 5A–F). The qPCR confirmed that CCS, WCS and

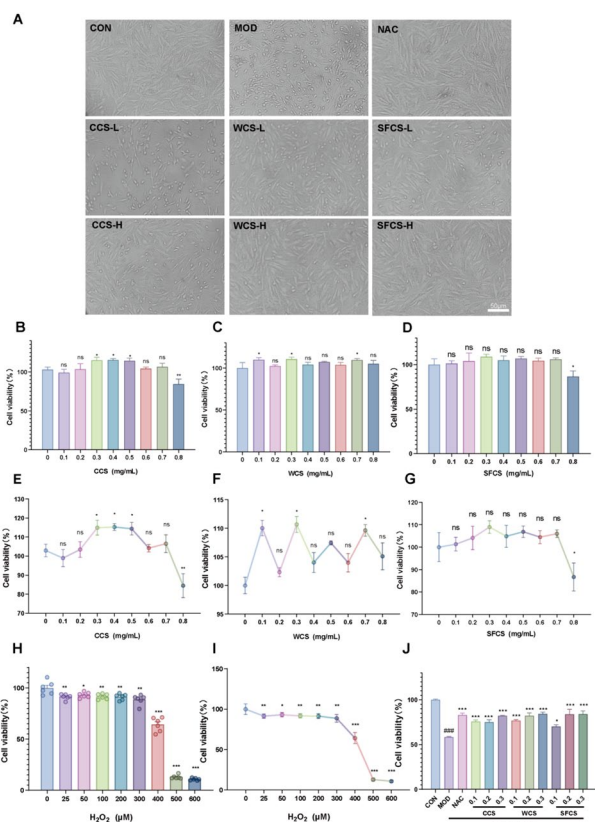


**Fig. 2** CCS, WCS, and SFCS mitigated injury to H<sub>2</sub>O<sub>2</sub>-challenged KGN cells. **A** Photographs of untreated KGN cells and those treated with CCS, WCS, SFCS, NAC, and H<sub>2</sub>O<sub>2</sub>. **B–J** Effect of CCS, WCS, SFCS, NAC, and H<sub>2</sub>O<sub>2</sub> on KGN cell viability. **D** Effect of CCS on KGN cell viability. Data are means ± standard deviation (S.D.) (n ≥ 3). ###P < 0.001 vs. CON group; \*P < 0.05, \*\*P < 0.01, \*\*\*P < 0.001 vs. MOD group; ns, not significantly different from the MOD group

SFCS downregulated Bax mRNA and upregulated Bcl-2 mRNA (Fig. 6A–C). WCS and SFCS were more effectively anti-apoptotic at 0.3 mg/mL than at 0.1 mg/mL.

**CCS, WCS and SFCS activate the Keap1-Nrf2/HO-1 pathway in H<sub>2</sub>O<sub>2</sub>-challenged KGN cells**

The Keap1-Nrf2 antioxidant response element (ARE) signaling pathway regulates the transcription of various antioxidant genes [31]. Figure 8A–F show that H<sub>2</sub>O<sub>2</sub> challenge upregulated Keap 1 protein and downregulated Nrf2, HO-1, SOD2, and NQO1 proteins. CCS, WCS and SFCS pretreatment had the opposite effects. The qPCR verified showed that CCS, WCS and SFCS pretreatment downregulated Keap1 mRNA and upregulated Nrf2, HO-1, CAT, SOD1, and NQO1 mRNA (Fig. 7A–F). The foregoing results suggest that CCS, WCS and SFCS inhibit the oxidative stress response in H<sub>2</sub>O<sub>2</sub>-challenged KGN cells by activating the Keap1-Nrf2/HO-1 pathway. Furthermore, WCS and SFCS more effectively

counteracted the effects of oxidative stress than CCS. Thus, wine processing and stir-frying enhance the antioxidant efficacy of CS.

**Effects of CCS, WCS and SFCS on the PI3K-Akt pathway in H<sub>2</sub>O<sub>2</sub>-challenged KGN cells**

Numerous cellular stimuli and toxic insults activate the PI3K-Akt signaling pathway. PI3K catalyzes phosphatidylinositol-3,4,5-triphosphate (PIP3) biosynthesis in the cell membrane. In turn, PIP3 is a secondary messenger that activates Akt. The latter controls apoptosis, protein synthesis, metabolism, and the cell cycle by phosphorylating certain substrates associated with these processes [32]. Figure 9A–G show that the P-PI3K and P-Akt proteins were downregulated in H<sub>2</sub>O<sub>2</sub>-challenged KGN cells. Pretreatments with 0.1 mg/mL and 0.3 mg/mL CCS, WCS and SFCS upregulated P-PI3K and P-Akt in a dose-dependent manner. Nevertheless, there was no significant difference in total Akt or PI3K protein content. Hence, CCS, WCS and SFCS promote PI3K and Akt phosphorylation and activate the PI3K-Akt signaling pathway in KGN cells. However, 0.3 mg/mL WCS and SFCS were relatively more effective at inducing the PI3K-Akt signaling pathway in H<sub>2</sub>O<sub>2</sub>-challenged KGN cells than either CCS or the lower concentrations of WCS and SFCS.

**Discussion**

Comprehensive research conducted over the past two decades has demonstrated that oxidative stress contributes to the initiation and development of female reproductive diseases such as premature ovarian insufficiency (POI). The latter is the most common fertility disorder in women below reproductive age [33]. The association between POI and redox imbalance has been reported in an earlier study [34]. The KGN cell line is a widely used in vitro POI model as it physiologically resembles the immature granulosa cells obtained from smaller antral follicles [35]. Modern pharmacology has indicated that Cuscutae Semen (CS) reverses reductions in testosterone levels and androgen receptor gene expression, and is immunomodulatory, hepatoprotective, antioxidant, anti-inflammatory, and anti-aging. It also enhances memory by inducing PC12 cell differentiation [8, 36, 37]. Crude Cuscutae Semen (CCS), wine-processed CS (WCS), and stir-frying-processed CS (SFCS) have different clinical applications as processing has conferred a unique pharmaceutical effect upon each of them according to traditional Chinese medicine (TCM). The results of component analysis showed that flavonoids, phenolic acids and lignans were the main differences between CCS, WCS and SFCS. The results were summarized in Fig. 1 and Table 2, which showed that the content and species



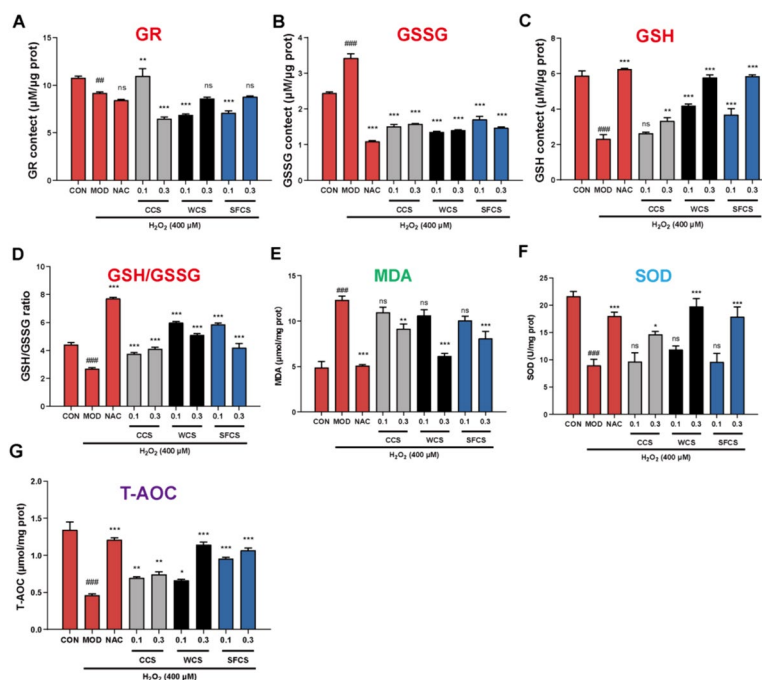


**Fig. 3** CCS, WCS, and SFCS offset redox imbalance in  $H_2O_2$ -challenged KGN cells. **A** GR levels in KGN cells. **B** GSSG levels in KGN cells. **C** GSH levels in KGN cells. **D** GSH/GSSG ratios in KGN cells. **E** MDA levels in KGN cells. **F** SOD levels in KGN cells. **G** T-AOC levels in KGN cells. Data are means  $\pm$  S.D. ( $n \geq 3$ ). ### $P < 0.001$ , ## $P < 0.01$  vs. CON group; \* $P < 0.05$ , \*\* $P < 0.01$ , \*\*\* $P < 0.001$  vs. MOD group; ns, not significantly different from the MOD group

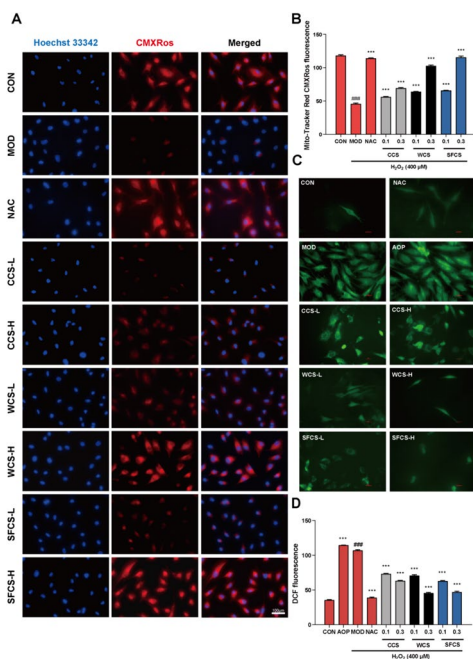


**Fig. 4** CCS, WCS, and SFCS increased mitochondrial activity in  $H_2O_2$ -challenged KGN cells. **A** Mitochondrial membrane potentials (MMP) in KGN cells were measured by CMXRos staining and fluorescence microscopy. **B** Quantification of CMXRos fluorescence. **C** ROS levels in KGN cells were measured by staining with DCFH-DA and fluorescence microscopy. **D** Quantification of DCF fluorescence. Data are means  $\pm$  S.D. ( $n \geq 3$ ). ### $P < 0.001$  vs. CON group; \*\*\* $P < 0.001$  vs. MOD group

of flavonoids changed greatly after wine-processed and stir-frying-processed.

However, few studies have been conducted on the therapeutic efficacy of CCS, WCS and SFCS against POI. To the best of our knowledge, the present study is one of the first to show that CCS, WCS and SFCS ameliorate apoptosis and oxidative stress in  $H_2O_2$ -challenged KGN cells by activating the Nrf2-Keap 1 signaling pathway and PI3K-Akt phosphorylation. Here, all concentrations of CCS, WCS and SFCS somewhat protected the KGN cells against  $H_2O_2$ -induced oxidative injury. Nevertheless, the antioxidant activity levels of WCS and SFCS were higher than that of CCS (Fig. 2). However, it remains to be determined whether WCS and SFCS have stronger antioxidant efficacy than CCS in  $H_2O_2$ -challenged KGN cells.

$H_2O_2$  exposure overloads cellular reactive oxygen species (ROS), depletes cellular reduced glutathione (GSH) pools, induces malondialdehyde (MDA) biosynthesis, and ultimately causes cell death [38]. Glutathione reductase (GR; EC 1.6.4.2) is a flavoprotein oxidoreductase that catalyzes the reduction of oxidized glutathione (GSSG) to GSH [39]. Here, we found that CCS, WCS and SFCS pretreatment decreased intracellular ROS levels in a dose-dependent manner (Fig. 4C and D). We also discovered that  $H_2O_2$  exposure disrupted redox homeostasis because it increased MDA and GSSG and decreased SOD, T-AOC, GSH, GR, and GSH/GSSG. As NAC,

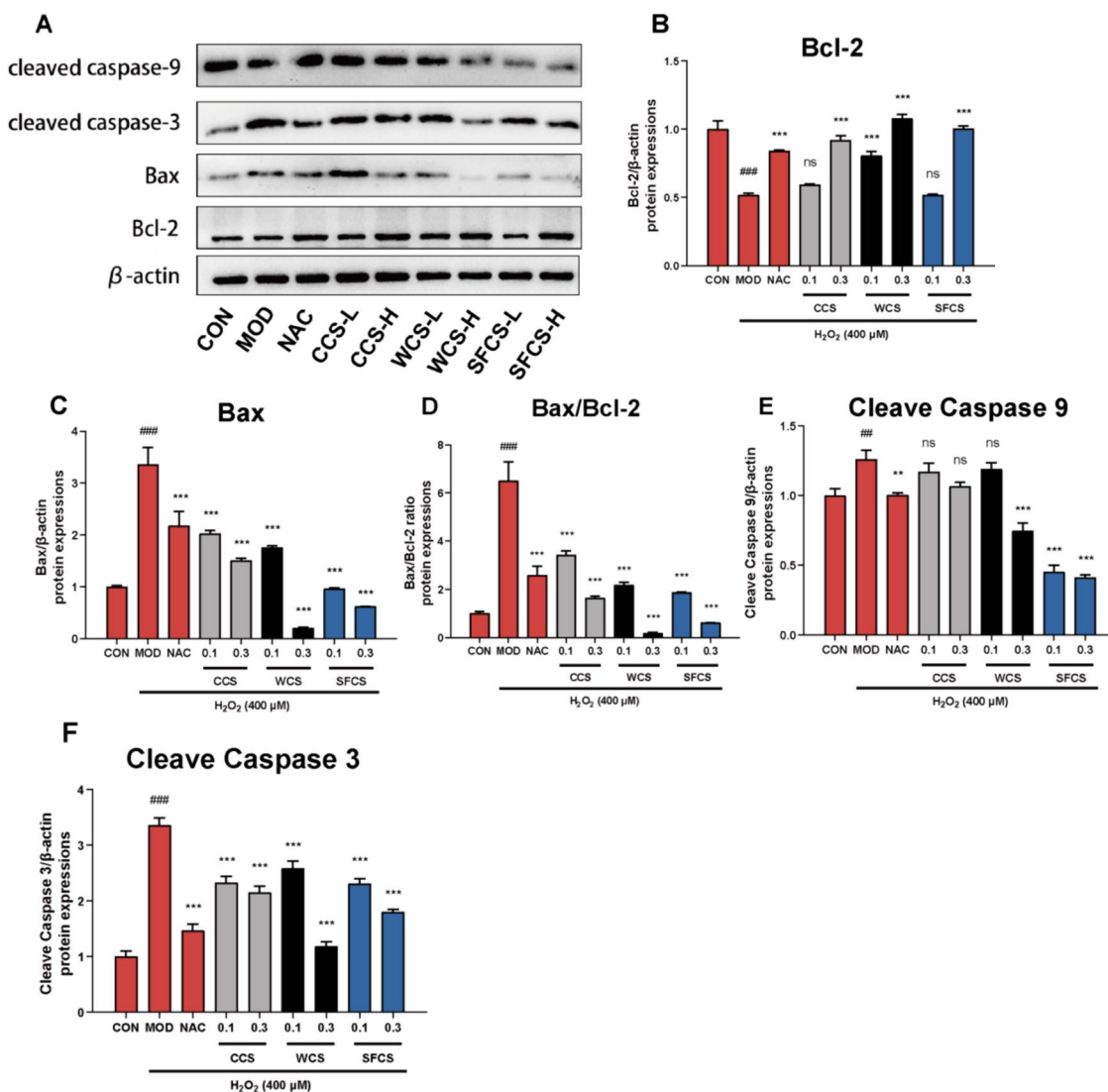


**Fig. 5** Regulation of apoptosis-related protein levels by CCS, WCS, and SFCS in H<sub>2</sub>O<sub>2</sub>-challenged KGN cells. **A–F** Bcl-2, Bax, cleaved caspase 9, and cleaved caspase 3 protein levels and Bax/Bcl-2 ratios in KGN cells treated with CCS, WCS, and SFCS in the presence or absence of H<sub>2</sub>O<sub>2</sub> treatment. Protein expression was normalized against β-actin. Data are means ± S.D. (n ≥ 3). ###P < 0.001, #P < 0.01 vs. CON group; \*\*P < 0.01, \*\*\*P < 0.001 vs. MOD group; ns, not significantly different from the MOD group

CCS, WCS and SFCS partially reversed these abnormal changes, they might augment the ability of antioxidants to eliminate free radicals (Fig. 3). Taken together, the results of the present work suggest that although CCS, WCS and SFCS effectively alleviated oxidative stress in H<sub>2</sub>O<sub>2</sub>-challenged KGN cells, WCS and SFCS had superior efficacy to CCS.

ROS accumulation may cause oxidative stress leading to granulosa cell apoptosis, oocyte deterioration, and, by extension, reduced fertility [40]. Figure 2A shows that exposure to 400 μM H<sub>2</sub>O<sub>2</sub> significantly increased the number of apoptotic cells. CCS, WCS and SFCS

pretreatment significantly decreased apoptosis in a dose-dependent manner compared to the MOD group. The mitochondria-mediated intrinsic apoptotic pathway is triggered by a variety of endogenous or exogenous stimuli, including DNA damage, oxidative or endoplasmic reticulum stress, ischemia, and more. This pathway begins with the disruption of the mitochondrial membrane potential (MMP), which is followed by the release of cytochrome C and other proapoptotic proteins, the formation of an apoptosome, and ultimately, apoptosis. [41] The MMP collapses early in apoptosis [42]. This phenomenon was observed in the H<sub>2</sub>O<sub>2</sub>-challenged KGN

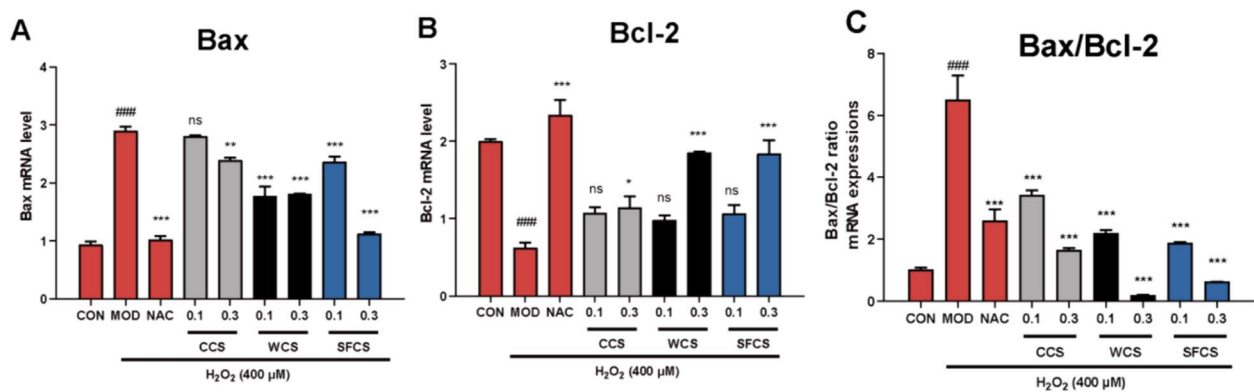


**Fig. 6** Regulation of apoptosis-related gene levels by CCS, WCS, and SFCS in  $H_2O_2$ -challenged KGN cells. **A–C** Bcl-2 and Bax gene expression and Bax/Bcl-2 ratios in response to CCS, WCS, and SFCS in the presence or absence of  $H_2O_2$  treatment. Gene expression was normalized against  $\beta$ -actin. Data are means  $\pm$  S.D. ( $n \geq 3$ ). ### $P < 0.001$  vs. CON group; \* $P < 0.05$ , \*\* $P < 0.01$ , \*\*\* $P < 0.001$  vs. MOD group; ns, not significantly different from the MOD group

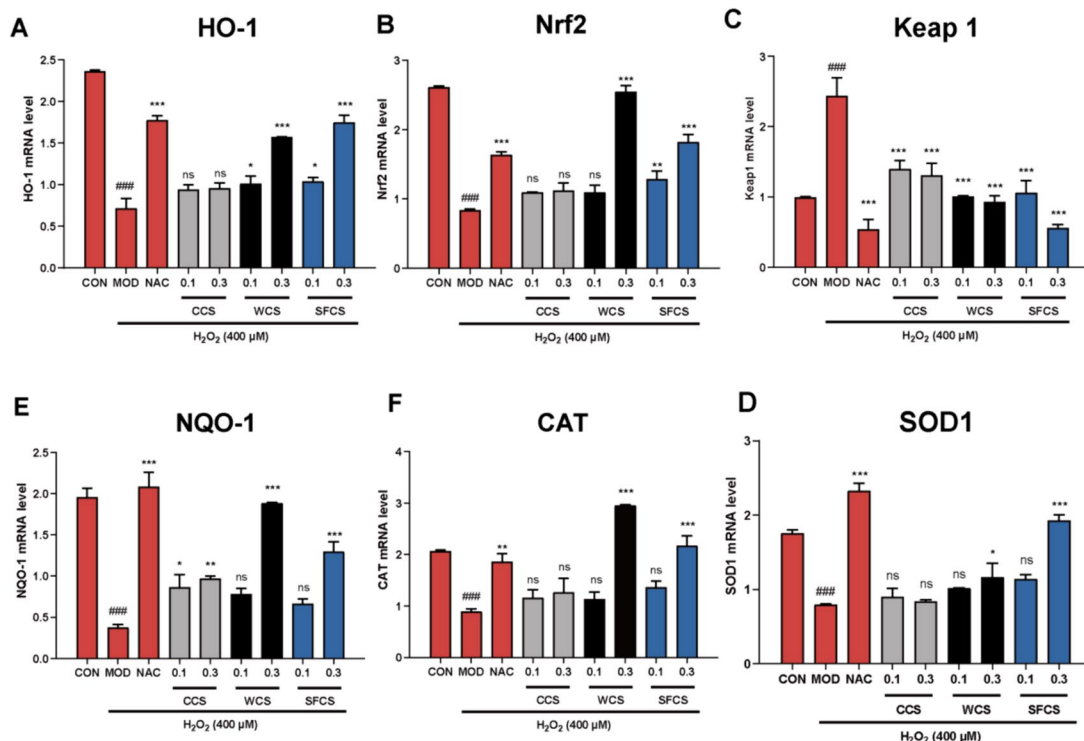


**Fig. 7** Effects of CCS, WCS, and SFCS on Nrf2-mediated antioxidant signaling transcripts were analyzed by qPCR. **A–F** HO-1, Nrf2, Keap1, SOD1, CAT, and NQO-1 gene expression levels in response to CCS, WCS, and SFCS in the presence or absence of  $H_2O_2$  treatment. Gene expression was normalized against  $\beta$ -actin. Data are means  $\pm$  S.D. ( $n \geq 3$ ). ### $P < 0.001$  vs. CON group; \* $P < 0.05$ , \*\* $P < 0.01$ , \*\*\* $P < 0.001$  vs. MOD group; ns, not significantly different from the MOD group

cells. CCS, WCS and SFCS modulated apoptosis-related gene and protein expression (Figs. 5 and 6). Bcl-2 and Bax regulate apoptosis [43]. The Bax/Bcl-2 ratio determines the rate of this process [44] and cleaves and activates the apoptosis mediator cleaved caspase-9. The latter then cleaves and activates the apoptosis executor

cleaved caspase-3 [45]. Here, CCS, WCS and SFCS significantly inhibited Bax, promoted Bcl-2, lowered the Bax/Bcl-2 ratio, and decreased the expression levels of cleaved caspase-9 and cleaved caspase-3 proteins. Figure 4A and B show that  $H_2O_2$  treatment reduces MMP and aggravates apoptosis in KGN cells whereas CCS,

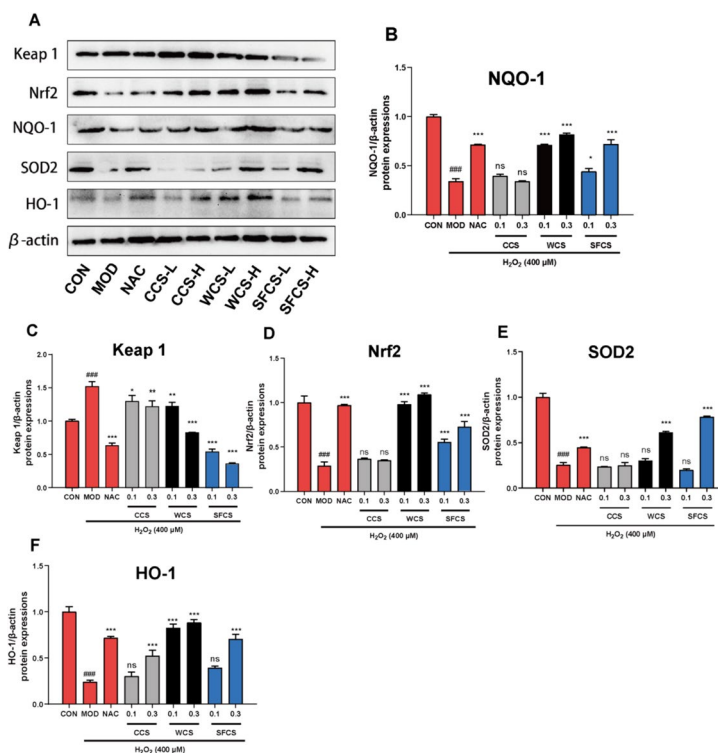


**Fig. 8** CCS, WCS, and SFCs regulate the Keap1/Nrf2 pathway in H<sub>2</sub>O<sub>2</sub>-challenged KGN cells. **A–F** NQO-1, Keap 1, Nrf2, SOD2, and HO-1 protein expression levels in response to CCS, WCS, and SFCs in the presence or absence of H<sub>2</sub>O<sub>2</sub> treatment. Protein expression was normalized against β-actin. Data are means ± S.D. (n ≥ 3). ###P < 0.001 vs. CON group; \*P < 0.05, \*\*P < 0.01, \*\*\*P < 0.001 vs. MOD group; ns, not significantly different from the MOD group

WCS and SFCs partially reverse these changes. Hence, CCS, WCS and SFCs inhibit MMP loss and apoptosis in H<sub>2</sub>O<sub>2</sub>-challenged KGN cells via a mechanism involving Bcl-2, Bax, cleaved caspase-9, and cleaved caspase-3. As WCS and SFCs exerted these effects more strongly than CCS, however, the former two have greater anti-apoptotic efficacy than the latter in H<sub>2</sub>O<sub>2</sub>-challenged KGN cells.

The transcription factor (TF) Nrf2 regulates cellular oxidative stress [46, 47]. Under steady-state, it is localized mainly to the cytoplasm at a low basal protein level as it undergoes Keap1-mediated proteasomal degradation. During oxidative stress, electrophiles and ROS inactivate Keap 1 and liberate Nrf2 from the Nrf2-Keap1 complex. Thence, Nrf2 is translocated to the nucleus where it binds the antioxidant response element (ARE) and induces downstream antioxidant proteins such as HO-1 and NQO1 [46]. SOD1 is localized mainly to the cytosol whereas the mitochondrial antioxidant enzyme SOD2 detoxifies superoxide anion generated during oxidative phosphorylation [48]. Nrf2 activation ameliorates mitochondrial dysfunction and alleviates oxidative stress and aberrant hormone secretion in the ovaries [49]. The current study aimed to establish whether the Keap1-Nrf2/

HO-1 pathway is implicated in the protective effects of CCS, WCS and SFCs on KGN cells. The western blot revealed that H<sub>2</sub>O<sub>2</sub> exposure weakly upregulated Nrf2 in the KGN cells whereas CCS, WCS and SFCs down-regulated Keap1 protein, strongly upregulated Nrf2, and promoted the nuclear translocation of the latter. CCS, WCS and SFCs also upregulated the antioxidant proteins HO-1, NQO1, and SOD2 (Fig. 8). The qPCR disclosed that CCS, WCS and SFCs also downregulated Keap1 mRNA but upregulated Nrf2, HO-1, CAT, SOD1, and NQO1 mRNA (Fig. 7). Altogether, these results demonstrated that CCS, WCS and SFCs alleviates apoptosis and oxidative stress via upregulation of Keap1-Nrf2/HO-1 signaling pathway-mediated antioxidant proteins, WCS and SFCs have a stronger effect on this pathway than CCS.

The PI3K/Akt signaling pathway regulates cell growth, proliferation, migration, invasion, apoptosis, and differentiation [50]. However, the pathway participating in Nrf2 induction is unknown. Earlier studies showed that the PI3K/Akt signaling pathways are involved in the upstream Nrf2 signal [51, 52]. Here, PI3K and Akt protein expression remain relatively unchanged. CCS, WCS and SFCs activated the PI3K/Akt pathway by upregulating

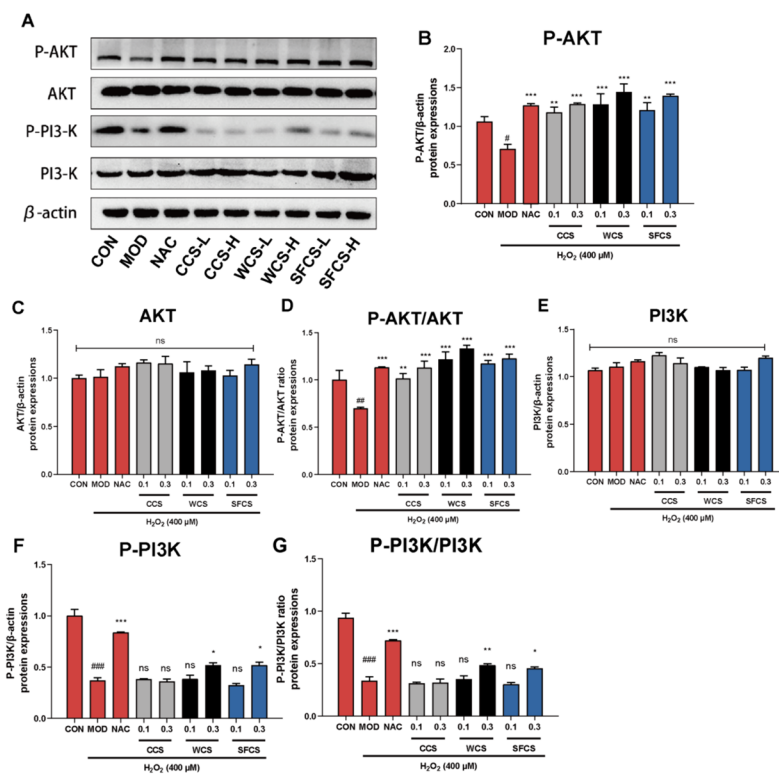


**Fig. 9** CCS, WCS, and SFCS regulate the Akt/PI3K pathway in H<sub>2</sub>O<sub>2</sub>-challenged KGN cells. **A–G** Akt, P-Akt, PI3K, and P-PI3K protein expression levels and P-Akt/Akt and P-PI3K/PI3K ratios in KGN cells treated with CCS, WCS, and SFCS in the presence or absence of H<sub>2</sub>O<sub>2</sub> treatment. Protein expression was normalized against β-actin. Data are means ± S.D. (n ≥ 3). #P < 0.05, ##P < 0.01, ###P < 0.001 vs. CON group; \*P < 0.05, \*\*P < 0.01, \*\*\*P < 0.001 vs. MOD group; ns, not significantly different from the MOD group

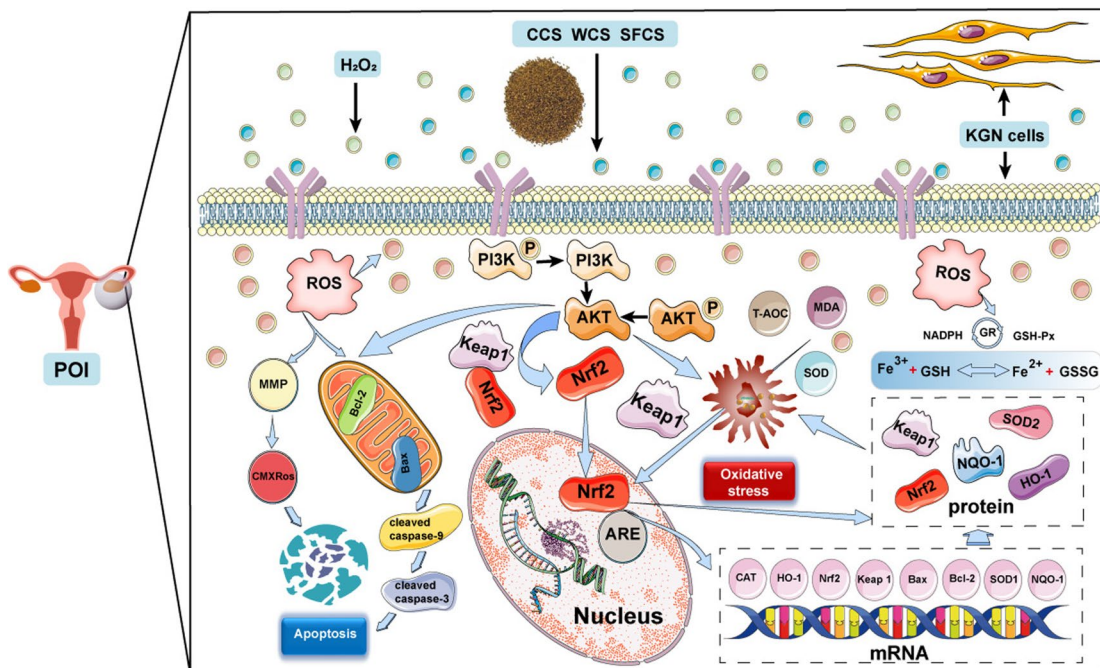


**Fig. 10** Mechanisms diagram of protective effects of CCS, WCS, SFCS in H<sub>2</sub>O<sub>2</sub>-induced KGN cells. CCS, WCS and SFCS inhibited apoptosis and oxidative stress in KGN cells subjected to H<sub>2</sub>O<sub>2</sub> by activating the PI3K/Akt-mediated Keap1-Nrf2/HO-1 signaling pathway

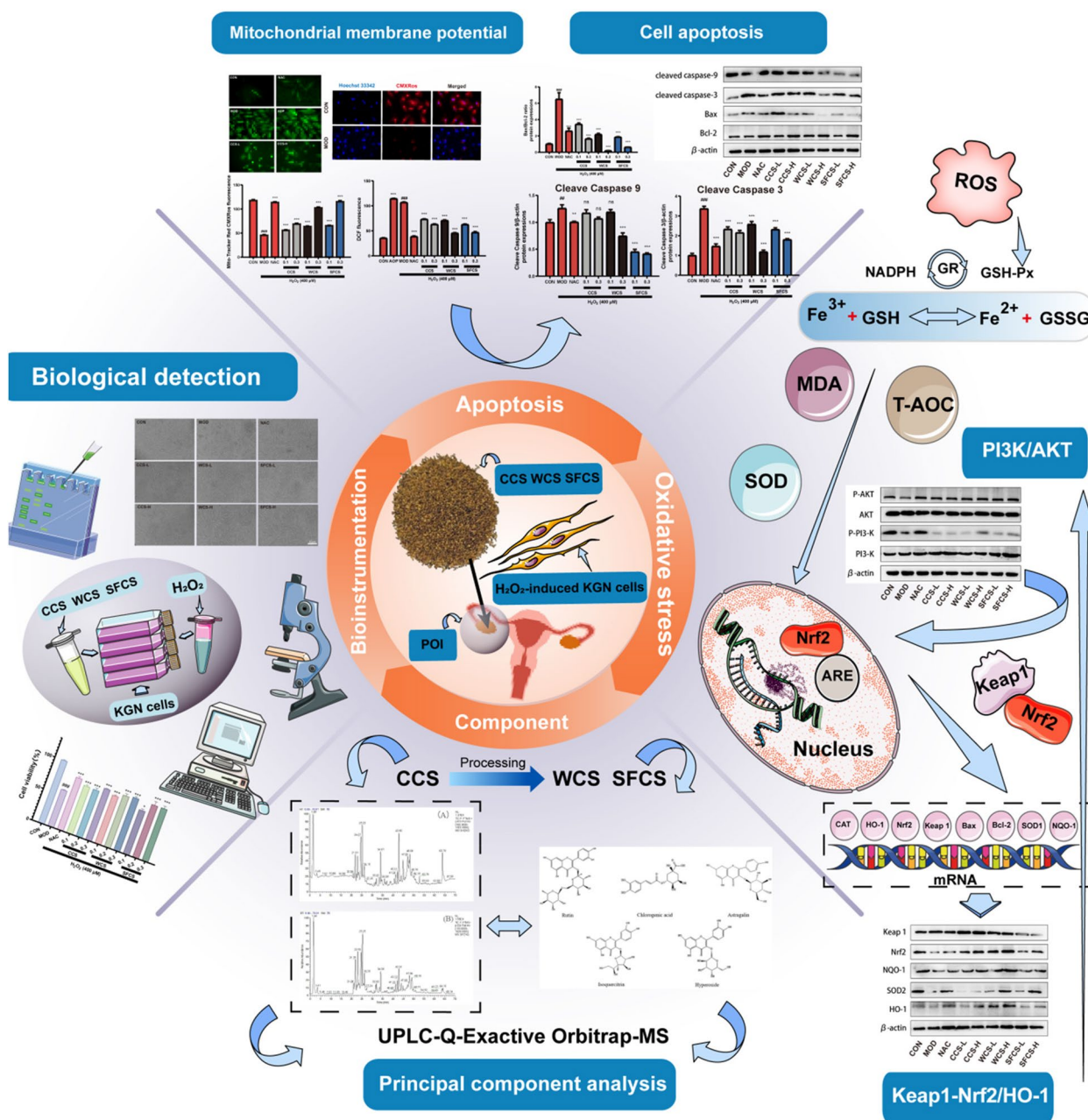


**Fig. 11** Graphical abstract

P-Akt and P-PI3K protein expression (Fig. 9). Thus, these results indicated PI3K/Akt signaling pathway activation as the upstream signal stimulating Keap1-Nrf2/HO-1 in CCS, WCS and SFCS-treated POI cell model. Therefore, CCS, WCS and SFCS may have protected KGN cells against H<sub>2</sub>O<sub>2</sub>-induced oxidative stress by activating the PI3K-Akt signaling pathway in a dose-dependent manner,

and WCS and SFCS were more effective than CCS in this regard.

**Conclusion**

To the best of our knowledge, as shown in Figs. 10 and 11, the present study was one of the first to indicate that CCS, WCS and SFCS inhibited apoptosis and oxidative

stress in KGN cells subjected to H<sub>2</sub>O<sub>2</sub> by activating the PI3K/Akt-mediated Keap1-Nrf2/HO-1 signaling pathway. Moreover, this work showed that WCS and SFCS had superior efficacy to CCS in POI therapy and suggest that the relative efficacies of these formulations against this disorder should be evaluated using the appropriate in vivo models. Based on the study of POI, it is also possible to conduct ex vivo and in vivo binding studies of the common active monomer components of CCS, WCS and SFCS.

## Supplementary Information

The online version contains supplementary material available at <https://doi.org/10.1186/s12906-024-04491-5>.

Supplementary Material 1.

Supplementary Material 2.

## Acknowledgements

Not applicable.

## Authors' contributions

Conceptualization, Y.L., Y.S., R.G. and C.X.; methodology, Y.L., Y.S., W.L., and K.Q.; software, Y.L. and R.G.; validation, Y.L., X.G., W.L., and K.Q.; formal analysis, Y.L., Y.S., R.G., C.X., M.F., and J.S.; investigation, Y.L., Y.S., R.G., C.X., M.F., and J.S.; resources, X.G., W.L. and K.Q.; data curation, Y.L., Y.S. and R.G.; writing—original draft preparation, Y.L., Y.S. and R.G.; writing—review and editing, Y.L., Y.S., R.G. and K.Q.; visualization, Y.L., Y.S., R.G., C.X., M.F., J.S., X.G., W.L. and K.Q.; supervision, K.Q.; project administration, X.G. and W.L.; funding acquisition, X.G., W.L. and K.Q.; All authors have read and agreed to the published version of the manuscript.

## Funding

The authors would like to thank the National Nature Science Foundation of China (No. 82374038), Major Projects of Natural Science Foundation of Jiangsu Higher Education Institutions (No. 21KJA360005) and a Project Funded by the Priority Academic Program Development of Jiangsu Higher Education Institutions (PAPD) for the financial support to this research.

## Availability of data and materials

The datasets during and/or analysed during the current study available from the corresponding author on reasonable request.

## Declarations

## Ethics approval and consent to participate

Not applicable.

## Consent for publication

Not applicable.

## Competing interests

The authors declare no competing interests.

## Author details

<sup>1</sup>School of Pharmacy, Jiangsu Ocean University, Lianyungang 222005, China.

<sup>2</sup>Department of Pharmacy, Xinyi People's Hospital, Xinyi Jiangsu 221400, China.

<sup>3</sup>Engineering Research Center of State Ministry of Education for Standardization of Chinese Medicine Processing, Nanjing University of Chinese Medicine, Nanjing 210023, China.

Received: 7 December 2023 Accepted: 7 May 2024

Published online: 15 May 2024

## References

- Webber L, Davies M, Anderson R, Bartlett J, Braat D. ESHRE Guideline: management of women with premature ovarian insufficiency. Hum Reprod. 2016;31:926–37.
- Laurinda A, Jeremy R. Regulation of mammalian oocyte meiosis by intercellular communication within the ovarian follicle. Annu Rev Physiol. 2017;79:237–60.
- Julia R, Alcoba D, Brum I, Dietrich J, Berthe Y, Katrin H, et al. FMR1 expression in human granulosa cells increases with exon 1 CGG repeat length depending on ovarian reserve. Reprod Biol Endocrinol. 2018;16:65–73.
- Yang S, Xu H, Zhao B, Li S, Li T, Xu X, et al. The difference of chemical components and biological activities of the crude products and the salt-processed product from semen cuscutae. Evid Based Complement Altern Med. 2016;2016:1–9.
- Shi Y, Jin J, Xu C, Liang Y, Liu X, Gao X, et al. Simultaneous quantitative analyses of five constituents in crude and salt-processed Cuscutae Semen using a validated high-performance thin-layer chromatography method. JPC-J Planar Chromat. 2022;35:421–30.
- Lin M, Lee M, Chang W, Yang M, Chu C. AN-P35 Study the immunomodulatory activity of Semen cuscutae and identify the active components (Section I Animal and Plant Cell Cultures). J Biosci Bioeng. 2009;108:S4–20.
- Yen F, Wu T, Lin L, Lin C. Hepatoprotective and antioxidant effects of cuscuta chinensis against acetaminophen-induced hepatotoxicity in rats. J Ethnopharmacol. 2007;111:123–8.
- Liu J, Jiang B, Bao Y, An L. Effect of *Cuscuta chinensis* glycoside on the neuronal differentiation of rat pheochromocytoma PC12 cells. Int J Dev Neurosci. 2003;21:277–81.
- Gao F, Zhou C, Qiu W, Wu H, Li J, Peng J, et al. Total flavonoids from semen cuscutae target MMP9 and promote invasion of EVT cells via Notch/AKT/MAPK signaling pathways. Sci Rep. 2018;8:17342–51.
- Xu C, Shi Y, Xu H, Zhao G, Niu S, Yao J, et al. Comparative investigation between raw and stir-frying processed cuscutae semen based on HPLC fingerprints coupled with chemometric methods. J AOAC Int. 2023;106:1037–47.
- Su C, Zhang R, Zhang X, Lv M, Liu X, Ao K, et al. Dingkun Pill modulate ovarian function in chemotherapy-induced premature ovarian insufficiency mice by regulating PTEN/PI3K/AKT/FOXO3a signaling pathway. J Ethnopharmacol. 2023;315:116703–14.
- Pi X, Xie L, Portbury A, Kumar S, Lockyer P, Li X, et al. NADPH oxidase-generated reactive oxygen species are required for stromal cell-derived factor-1-stimulated angiogenesis. Arterioscler Thromb Vasc Biol. 2014;34:2023–32.
- Rendra E, Riabov V, Mossel D, Sevastyanova T, Harmsen M, Kzhyshkowska J. Reactive oxygen species (ROS) in macrophage activation and function in diabetes. Immunobiology. 2019;224:242–53.
- Lu S, Liao Z, Lu X, Katschinski D, Bers D. Hyperglycemia acutely increases cytosolic reactive oxygen species via o-linked GlcNAcylation and CaMKII activation in mouse ventricular myocytes. Circ Res. 2020;126:e80–96.
- Chen Y, Qin C, Huang J, Tang X, Liu C, Huang K, et al. The role of astrocytes in oxidative stress of central nervous system: A mixed blessing. Cell Prolif. 2020;53:e12781–93.
- Kumar M, Pathak D, Venkatesh S, Kriplani A, Ammini A, Dada R. Chromosomal abnormalities & oxidative stress in women with premature ovarian failure (POF). Indian J Med Res. 2012;135:92–7.
- Tokmak A, Yldrm G, Sarkaya E, Nar M, Yilmaz N. Increased oxidative stress markers may be a promising indicator of risk for primary ovarian insufficiency: a cross-sectional case control study. Rev Bras Ginecol Obstet. 2015;37:411–6.
- Liu T, Liu Y, Huang Y, Chen J, Lai L. MiR-15b induces premature ovarian failure in mice via inhibition of α-Klotho expression in ovarian granulosa cells. Free Radical Biol Med. 2019;141:383–92.
- Nishi Y, Yanase T, Mu Y, Oba K, Lchino I, Saito M, et al. Establishment and characterization of a steroidogenic human granulosa-like tumor cell line, KGN, that expresses functional follicle-stimulating hormone receptor. Endocrinology. 2001;142:437–45.
- Liu J, Shi D, Ma Q, Zhao P. Yangjing Zhongyu decoction facilitates mitochondrial activity, estrogenesis, and energy metabolism in H<sub>2</sub>O<sub>2</sub>-induced human granulosa cell line KGN. J Ethnopharmacol. 2022;295:115398–409.

21. Sies H. Oxidative stress: a concept in redox biology and medicine. *Redox Biol.* 2015;4:180–3.
22. Filomeni G, Zio D, Cecconi F. Oxidative stress and autophagy: The clash between damage and metabolic needs. *Cell Death Differ.* 2015;22:377–88.
23. Lzquierdoalonso J, Pérezrial S, Rivera C, Pecesbarba G. N-acetylcysteine for prevention and treatment of COVID-19: Current state of evidence and future directions. *J Infect Public Health.* 2022;15:1477–83.
24. Vatner S, Zhang J, Oydanch M, Berkman T, Vatner D. Healthful aging mediated by inhibition of oxidative stress. *Ageing Res Rev.* 2020;64:101194–246.
25. Cebula M, Schmidt E, Arnér E. TrxR1 as a potent regulator of the Nrf2-Keap1 response system. *Antioxid Redox Signal.* 2015;23:823–53.
26. Lin M, Xie W, Xiong D, Tang S, Huang X, Deng L, et al. Cyasterone ameliorates sepsis-related acute lung injury via AKT (Ser473)/GSK3 $\beta$  (Ser9)/Nrf2 pathway. *Chinese Medicine.* 2023;18:136–51.
27. Aleksandra K, Damian F, Forman H, Jozkowicz A, Grochot P. Beyond repression of Nrf2: An update on Keap1. *Free Radical Biol Med.* 2020;157:63–74.
28. Dodson M, Zhang D. Chronic arsenic-induced metabolic syndrome: a role for prolonged Nrf2 activation and mitochondrial metabolism. *Free Radical Biol Med.* 2016;100:5183.
29. Yang H, Lv H, Li H, Ci X, Peng L. Oridonin protects LPS-induced acute lung injury by modulating Nrf2-mediated oxidative stress and Nrf2-independent NLRP3 and NF- $\kappa$ B pathways. *Cell Communication and Signaling.* 2019;17:62–76.
30. Zhang Y, Ali K, Khan F, Yan S, Lhsan A, Ding Q. Chitosan oligosaccharides prevent doxorubicin-induced oxidative stress and cardiac apoptosis through activating p38 and JNK MAPK mediated Nrf2/ARE pathway. *Chem Biol Interact.* 2019;305:54–65.
31. Bellezza I, Giambanco I, Minelli A, Donato R. Nrf2-Keap1 signaling in oxidative and reductive stress. *Biochim Biophys Acta Mol Cell Res.* 2018;1865:721–33.
32. Hers I, Vincent E, Tavaré J. Akt signalling in health and disease. *Cell Signal.* 2011;23:1515–27.
33. Lu J, Wang Z, Cao J, Chen Y, Dong Y. A novel and compact review on the role of oxidative stress in female reproduction. *Reprod Biol Endocrinol.* 2018;16:80–97.
34. Yan F, Zhao Q, Li Y, Zheng Z, Kong X, Shu C, et al. The role of oxidative stress in ovarian aging: a review. *J Ovarian Res.* 2022;15:100–19.
35. Zhou X, Zhang J, Li Y, Chen Y, Wu X, Li X, et al. Advanced oxidation protein products induce G1/G0-Phase arrest in ovarian granulosa cells via the ROS-JNK/p38 MAPK-p21 pathway in premature ovarian insufficiency. *Oxid Med Cell Longev.* 2021;2021:1–19.
36. Liao J, Chang W, Lee M, Chiu Y, Peng W. Antinociceptive and anti-inflammatory activities of *Cuscuta chinensis* seeds in mice. *Am J Chin Med.* 2014;42:223–42.
37. Lin M, Lee M, Chang W, Chia M. Study the immunomodulatory activity of Semen *Cuscutae* and identify the active components. *J Biosci Bioeng.* 2009;108:54–20.
38. Mario M, Valerio R, Marcello D, Gerarda G, Andrea A, Carmelina L, et al. Role of oxidative stress in pathophysiology of nonalcoholic fatty liver disease. *Oxid Med Cell Longev.* 2018;2018:1–14.
39. Zhang P, Liu S, Chen K. Characterization and expression analysis of a glutathione reductase gene from antarctic moss *Pohlia nutans*. *Plant Mol Biol Report.* 2013;31:1068–76.
40. Sasaki H, Toshio H, Shintaro K, Maki I, Masato K, Seiji O, et al. Impact of oxidative stress on age-associated decline in oocyte developmental competence. *Front Endocrinol.* 2019;10:811–7.
41. Qureshi S, Lee S, Steidl W, Ritzer L, Parise M, Chaubal A, et al. Endoplasmic reticulum stress disrupts mitochondrial bioenergetics, dynamics and causes corneal endothelial cell apoptosis. *Invest Ophthalmol Vis Sci.* 2023;64:18–33.
42. Byun E, Cho E, Kim Y, Kim W, Byun E. Neuroprotective effect of polysaccharide separated from *Perilla frutescens* Britton var. *acuta* Kudo against H<sub>2</sub>O<sub>2</sub>-induced oxidative stress in HT22 hippocampus cells. *Biosci Biotechnol Biochem.* 2018;82:1344–58.
43. Song J, Shin M, Hwang G, Oh S, Hwang J, Kang K. Chebulinic acid attenuates glutamate-induced HT22 cell death by inhibiting oxidative stress, calcium influx and MAPKs phosphorylation. *Bioorg Med Chem Lett.* 2018;28:249–53.
44. Du L, Fei Z, Song S, Wei N. Antitumor activity of lobaplatin against esophageal squamous cell carcinoma through caspase-dependent apoptosis and increasing the Bax/Bcl-2 ratio. *Biomed Pharmacother.* 2017;95:447–52.
45. Budihardjo I, Oliver H, Lutter M, Xu L, Wang X. Biochemical pathways of caspase activation during apoptosis. *Annu Rev Cell Dev Biol.* 1999;15:269–90.
46. He F, Ru X, Wen T. NRF2, a transcription factor for stress response and beyond. *Int J Mol Sci.* 2020;21:4777–99.
47. Huang Q, Zhang C, Dong S, Han J, Qu S, Xie T, et al. Asafoetida exerts neuroprotective effect on oxidative stress induced apoptosis through PI3K/Akt/GSK3 $\beta$ /Nrf2/HO-1 pathway. *Chinese Medicine.* 2022;17:83–103.
48. Cyr A, Hitchler M, Domann F. Regulation of SOD2 in cancer by histone modifications and CpG methylation: closing the loop between redox biology and epigenetics. *Antioxid Redox Signal.* 2013;18:1946–55.
49. Luo M, Zheng L, Wang Y, Huang J, Yang Z, Yue Z, et al. Genistein exhibits therapeutic potential for PCOS mice via the ER-Nrf2-Foxo1-ROS pathway. *Food Funct.* 2021;12:8800–11.
50. Riescoezaguire G, Santisteban P. Molecular biology of thyroid cancer initiation. *Clin Transl Oncol.* 2007;9:686–93.
51. Jasekgajda E, Jurkowska H, Jasińska M, Lis G. Targeting the MAPK/ERK and PI3K/AKT signaling pathways affects NRF2, Trx and GSH antioxidant systems in leukemia cells. *Antioxidants.* 2020;9:633–50.
52. Tanaka M, Kishimoto Y, Sasaki M, Sato A, Kamiya T, Kondo K, et al. Terminalia bellirica (Gaertn.) Roxb. Extract and gallic acid attenuate LPS-induced inflammation and oxidative stress via MAPK/NF- $\kappa$ B and Akt/AMPK/Nrf2 pathways. *Oxid Med Cell Longev.* 2018;2018:9364364–78.

## Publisher's Note

Springer Nature remains neutral with regard to jurisdictional claims in published maps and institutional affiliations.